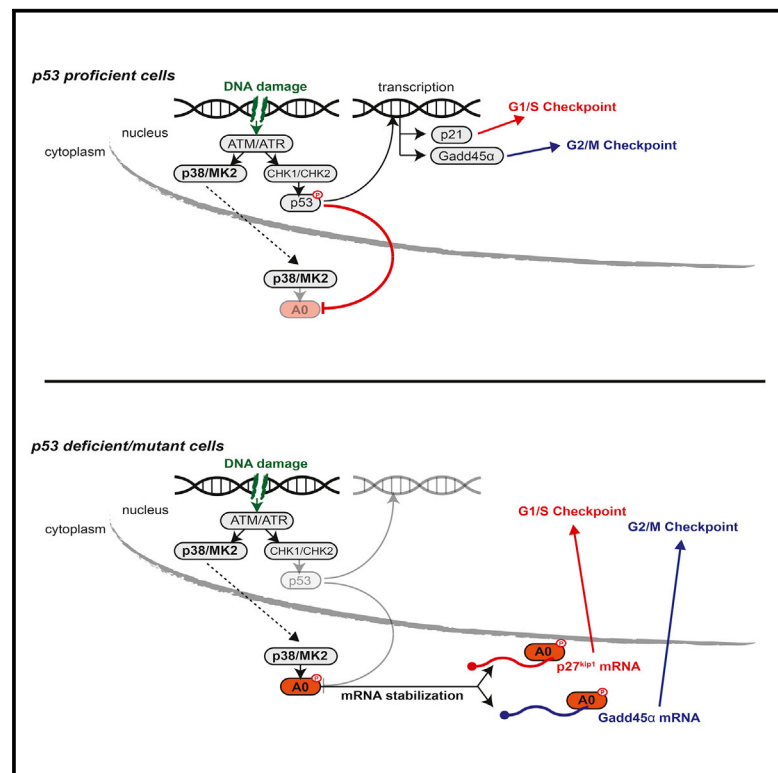


Cancer Cell

A Pleiotropic RNA-Binding Protein Controls Distinct Cell Cycle Checkpoints to Drive Resistance of p53-Defective Tumors to Chemotherapy

Graphical Abstract



Authors

Ian G. Cannell, Karl A. Merrick, Sandra Morandell, ..., Ming-Sound Tsao, Michael T. Hemann, Michael B. Yaffe

Correspondence

myaffe@mit.edu

In Brief

Cannell et al. show that NSCLC tumors with mutant p53 are critically dependent on the activity of a post-transcriptional MK2/hnRNPA0 pathway for resistance to chemotherapy. hnRNPA0 regulates both p27^{Kip1} and Gadd45α to enforce cell cycle checkpoints, allowing DNA repair and tolerance to chemotherapy.

Highlights

- p27 is an MK2/hnRNPA0 target controlling the G1/S checkpoint in p53-mutant cells
- hnRNPA0 drives chemo-resistance of p53-mutant tumor cells via p27/Gadd45α mRNAs
- Depleting hnRNPA0 enhances lung tumor response to cisplatin and prolongs survival
- RNA-binding proteins are critical components of the DNA damage response in vivo



A Pleiotropic RNA-Binding Protein Controls Distinct Cell Cycle Checkpoints to Drive Resistance of *p53*-Defective Tumors to Chemotherapy

Ian G. Cannell,¹ Karl A. Merrick,¹ Sandra Morandell,^{1,6} Chang-Qi Zhu,² Christian J. Braun,¹ Robert A. Grant,¹ Eleanor R. Cameron,¹ Ming-Sound Tsao,² Michael T. Hemann,¹ and Michael B. Yaffe^{1,3,4,5,*}

¹David H. Koch Institute for Integrative Cancer Research, Massachusetts Institute of Technology, Cambridge, MA 02139, USA

²Princess Margaret Cancer Centre, University Health Network and University of Toronto, Toronto, ON M5G 2M9, Canada

³Department of Biology, Massachusetts Institute of Technology, Massachusetts Institute of Technology, Cambridge, MA 02139, USA

⁴Department of Biological Engineering, Massachusetts Institute of Technology, Massachusetts Institute of Technology, Cambridge, MA 02139, USA

⁵Department of Surgery, Beth Israel Deaconess Medical Center, Harvard Medical School, Boston, MA 02215, USA

⁶Present address: Molecular Health, GmbH, 69115 Heidelberg, Germany

*Correspondence: myaffe@mit.edu

<http://dx.doi.org/10.1016/j.ccell.2015.09.009>

SUMMARY

In normal cells, p53 is activated by DNA damage checkpoint kinases to simultaneously control the G1/S and G2/M cell cycle checkpoints through transcriptional induction of p21^{cip1} and Gadd45 α . In *p53*-mutant tumors, cell cycle checkpoints are rewired, leading to dependency on the p38/MK2 pathway to survive DNA-damaging chemotherapy. Here we show that the RNA binding protein hnRNPA0 is the “successor” to p53 for checkpoint control. Like p53, hnRNPA0 is activated by a checkpoint kinase (MK2) and simultaneously controls both cell cycle checkpoints through distinct target mRNAs, but unlike p53, this is through the post-transcriptional stabilization of p27^{Kip1} and Gadd45 α mRNAs. This pathway drives cisplatin resistance in lung cancer, demonstrating the importance of post-transcriptional RNA control to chemotherapy response.

INTRODUCTION

Cytotoxic chemotherapy is a mainstay of cancer treatment, yet the molecular mechanisms that govern sensitivity or resistance to these agents in different tumor types are incompletely understood. Many of the most commonly used chemotherapeutic drugs exert their effects by causing DNA damage, leading to the activation of a complex signaling network that facilitates cell cycle arrest and/or cell death. During tumor evolution, however, many, if not all tumors disrupt components of the DNA damage response network (DDR) to escape oncogene-induced senescence (Bartkova et al., 2006), ultimately contributing to genomic instability. Cytotoxic anti-cancer chemotherapy works in large part by exploiting these DDR differences between normal

and tumor cells (Ciccia and Elledge, 2010; Jackson and Bartek, 2009). Some tumor types, such as testicular cancers, show a >80% response rate to chemotherapy (Kelland, 2007). In others, such as non-small cell lung cancer (NSCLC), however, only ~30% of patients respond favorably to cytotoxic platinum-based chemotherapy while the remaining ~70% receive little to no benefit and suffer from drug-related toxicity (Socinski, 2004). Hence, NSCLC is an ideal system to interrogate molecular mechanisms of intrinsic drug resistance. Importantly, the identification of chemotherapy resistance mechanisms could, in principle, both delineate new targets for pharmacological intervention and identify those patients most likely to benefit from specific therapeutic regimens while limiting the extent of toxicity associated with non-selective administration.

Significance

Platinum-containing regimens are frontline DNA-damaging therapies for non-small cell lung cancer (NSCLC), yet the molecular mechanisms that drive resistance to chemotherapy are incompletely understood. Here we show that NSCLC tumors with mutations in *p53* (~50%) are critically dependent on the activity of a post-transcriptional MK2/hnRNPA0 pathway for resistance to chemotherapy. hnRNPA0 regulates both p27^{Kip1} and Gadd45 α to enforce cell cycle checkpoints, allowing DNA repair and tolerance to chemotherapy. Analysis of hnRNPA0-target mRNAs in patients with NSCLC demonstrates that activity of this pathway correlates with therapeutic response. Thus, pre-screening of patients for the activity of the MK2/hnRNPA0 pathway may predict a sub-population of patients likely to benefit most from chemotherapy.

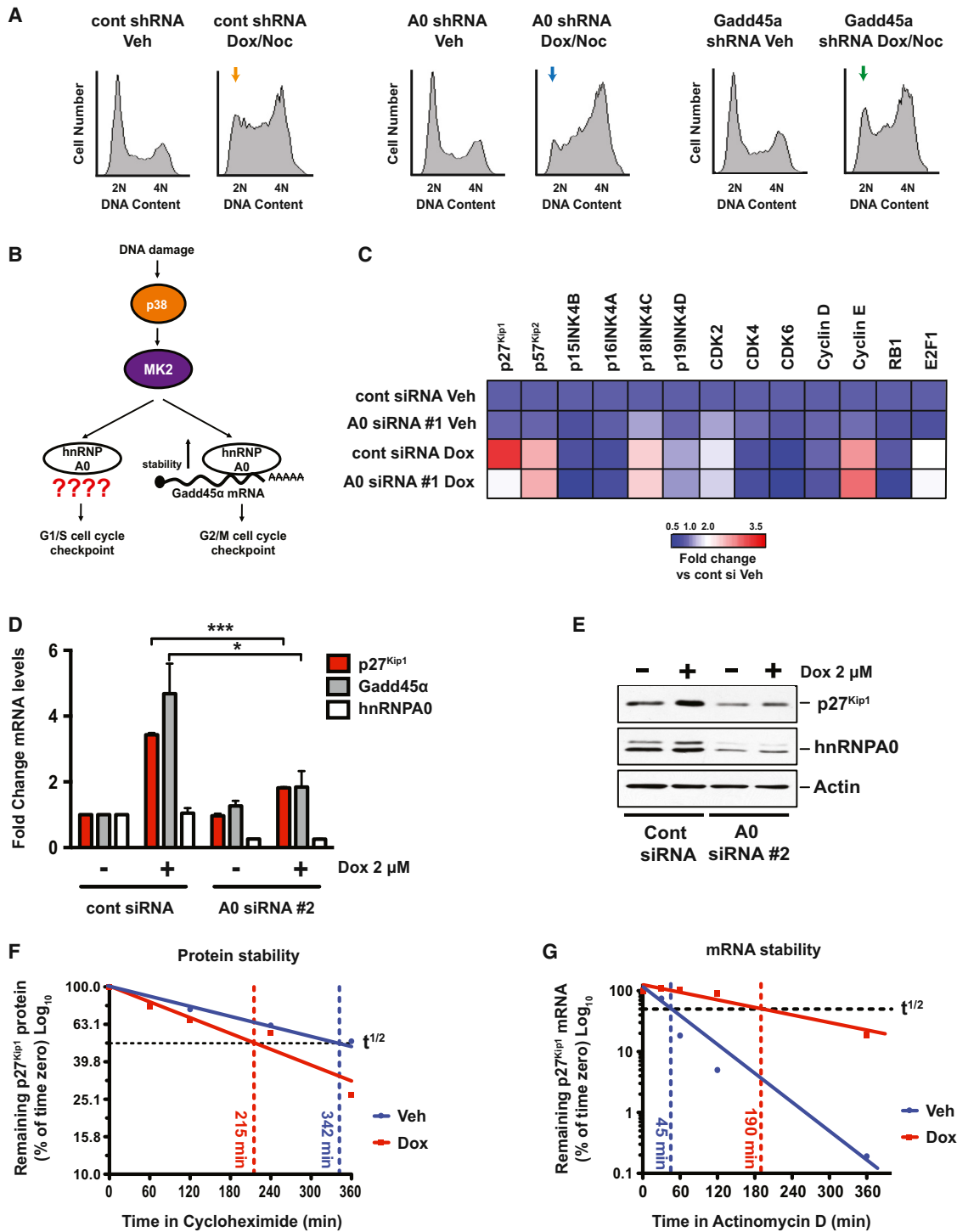


Figure 1. A Focused Screen Implicates p27^{Kip1} as an hnRNP A0-Dependent G1/S Regulator

(A) H1299 cells were depleted of hnRNP A0 or Gadd45 α and treated with 2 μ M doxorubicin for 4 hr followed by the addition of 250 ng/ml nocodazole for a further 24 hr. Cells were fixed and stained with propidium iodide and analyzed by flow cytometry. Yellow, blue, and green arrows depict loss of the G1/S checkpoint in hnRNP A0 knockdown cells but not in Gadd45 α knockdown cells.

(B) Schematic representation of the known role of hnRNP A0 in the DNA damage response.

(C) Cells were treated with doxorubicin for 16 hr, mRNA levels of the indicated targets were determined by qRT-PCR, and the data represented as fold-change versus control siRNA vehicle-treated cells.

(D) qRT-PCR analysis of H1299 cells, 16 hr post-doxorubicin treatment. Data are represented as fold change versus control siRNA vehicle-treated cells. Error bars represent mean \pm SEM, n = 3 experiments. *p < 0.05, ***p < 0.001.

(legend continued on next page)

Loss or mutation of the tumor suppressor *p53* occurs in approximately 50% of all tumors (Cheek et al., 2011). We recently demonstrated that *p53*-deficient cells and tumors become dependent on the *p38*/*MK2* pathway for survival in response to topoisomerase inhibitors or platinum-based compounds (Morandell et al., 2013; Reinhardt et al., 2007), two classes of commonly used chemotherapeutic agents. Those observations suggested that pharmacological targeting of *MK2*, or its downstream effectors, might promote greater clinical efficacy of chemotherapy in *p53*-deficient tumors (Morandell et al., 2013; Reinhardt et al., 2007). It is also possible that the activity of this pathway could be used to predict the efficacy of chemotherapy. However, measuring *MK2* expression levels or activation status as biomarkers of chemotherapy response is likely to be hampered by difficulties in directly assaying *MK2* activity in tumor cells, as well as the presence of high levels of *MK2* expression in tumor-infiltrating stromal cells such as macrophages (Morandell et al., 2013). A thorough mechanistic understanding of tumor-specific *MK2* effectors, however, could provide novel biomarkers that would facilitate the identification of subsets of patients most likely to benefit from chemotherapy.

We recently found that *MK2* post-transcriptionally controls the G2/M checkpoint through the RNA binding protein (RNA-BP) *hnRNPA0* promoting *Gadd45 α* mRNA stabilization and protein production (Reinhardt et al., 2010, 2011). In addition to loss of the G2/M checkpoint, *MK2* depleted *p53*-null cells also lose the DNA damage-induced G1/S checkpoint. The molecular mechanism underlying this G1/S checkpoint bypass, the relative contributions of different cell cycle checkpoints to chemotherapy sensitization, and the mechanistic basis for synthetic lethality between the *p53* and *MK2* pathways in response to DNA-damaging chemotherapy have remained elusive.

RESULTS

A Focused Screen Implicates *p27^{Kip1}* as an *hnRNPA0*-Dependent G1/S Regulator

As shown in Figure 1A, in addition to regulating the G2/M checkpoint, loss of *hnRNPA0* results in a pronounced loss of the DNA damage-induced G1/S checkpoint in *p53*-null H1299 NSCLC cells (see also Figure S1A). Depletion of *Gadd45 α* , the only known *hnRNPA0*-target mRNA involved in cell cycle control (Reinhardt et al., 2010), however, failed to recapitulate the effect of *hnRNPA0* knockdown on the G1/S checkpoint (Figure 1A, compare orange, blue and green arrows; see also Figure S1A), indicating that *hnRNPA0* must regulate the G1/S checkpoint through a different target mRNA(s) (Figure 1B). To identify putative *hnRNPA0*-target mRNAs that might control the G1/S checkpoint in these *p53*-deficient H1299 cells, we next performed a focused mRNA expression screen following *hnRNPA0* depletion, looking for altered regulation of mRNAs whose protein products have been implicated in regulating the

G1/S transition in different contexts (Figure 1C). Based on the assumption that *hnRNPA0* regulates the stability of its target mRNAs, as has been shown for *Gadd45 α* (Reinhardt et al., 2010), and thus their mRNA levels, we measured the expression of these G1/S regulators by qRT-PCR in cells depleted of *hnRNPA0* by RNAi in the presence or absence of doxorubicin-induced DNA damage. Treatment of H1299 cells with doxorubicin led to a number of changes in the mRNA levels of several G1/S regulators; however, only one of these mRNAs, *p27^{Kip1}*, appeared to be regulated in an *hnRNPA0*-dependent manner (Figure 1C). We confirmed this effect of *hnRNPA0* on *p27^{Kip1}* mRNA induction using a second independent siRNA targeting a second distinct sequence within *hnRNPA0*. This independent siRNA efficiently depleted *hnRNPA0* at both the mRNA (Figure 1D) and protein level (Figure 1E) and prevented the induction of both *p27^{Kip1}* and *Gadd45 α* mRNAs in response to DNA damage (Figure 1D). Furthermore, the marked induction of *p27^{Kip1}* protein levels that we observed after doxorubicin treatment was blunted by *hnRNPA0* knockdown (Figure 1E). Together these data indicate that a single RNA-binding protein, *hnRNPA0*, regulates the DNA damage-induced G1/S checkpoint independently of stabilizing *Gadd45 α* and that this G1/S checkpoint may instead be mediated by DNA damage-induced induction of *p27^{Kip1}*.

The most well-established mechanism for *p27^{Kip1}* regulation occurs at the level of protein stability through the action of the ubiquitin ligase *Skp2* (Frescas and Pagano, 2008). To investigate whether increased protein stability could account for the upregulation of *p27^{Kip1}* protein after DNA damage (Figure 1E), we measured *p27^{Kip1}* protein half-life after doxorubicin induced DNA damage by blocking translation with cycloheximide (Figures 1F and S1B). Surprisingly, despite a 2- to 3-fold increase in total *p27^{Kip1}* protein levels (Figure 1E), doxorubicin treatment led to a slight decrease in *p27^{Kip1}* protein stability (Figures 1F and S1B), indicating that the observed induction of *p27^{Kip1}* following DNA damage does not result from increased protein stability. Since *hnRNPA0* is known to regulate *Gadd45 α* in a DNA damage-dependent manner through stabilization of its mRNA (Reinhardt et al., 2010), we hypothesized that the increased *p27^{Kip1}* levels seen after DNA damage could be due to a similar stabilization of *p27^{Kip1}* mRNA. To test this, we treated H1299 cells with doxorubicin for 16 hr, then added actinomycin D to the culture medium to prevent new transcription and measured *p27^{Kip1}* mRNA decay by qRT-PCR. Doxorubicin treatment led to a fourfold increase in the half-life of *p27^{Kip1}* mRNA (Figure 1G), similar in magnitude to the observed increase in total *p27^{Kip1}* mRNA levels (Figures 1C and 1D). Next, we set out to examine whether the regulation of *p27^{Kip1}* by *hnRNPA0* is mediated by direct binding. In vitro binding experiments with a fragment of the *p27^{Kip1}* 3' UTR harboring putative *hnRNPA0* binding sites (Figure S1C) (Wang et al., 2013) and the purified recombinant *hnRNPA0* RNA recognition motifs (RRMs) (Figures S1D

(E) Western blots of H1299 cells 16 hr post-doxorubicin treatment.

(F) H1299 cells were treated with doxorubicin for 16 hr followed by the addition of cycloheximide. Samples were taken at indicated time points and *p27^{Kip1}* protein levels measured by immuno-blotting.

(G) H1299 cells were treated with doxorubicin for 16 hr followed by the addition of actinomycin D. At indicated time points, *p27^{Kip1}* mRNA levels were determined by qRT-PCR.

See also Figure S1.

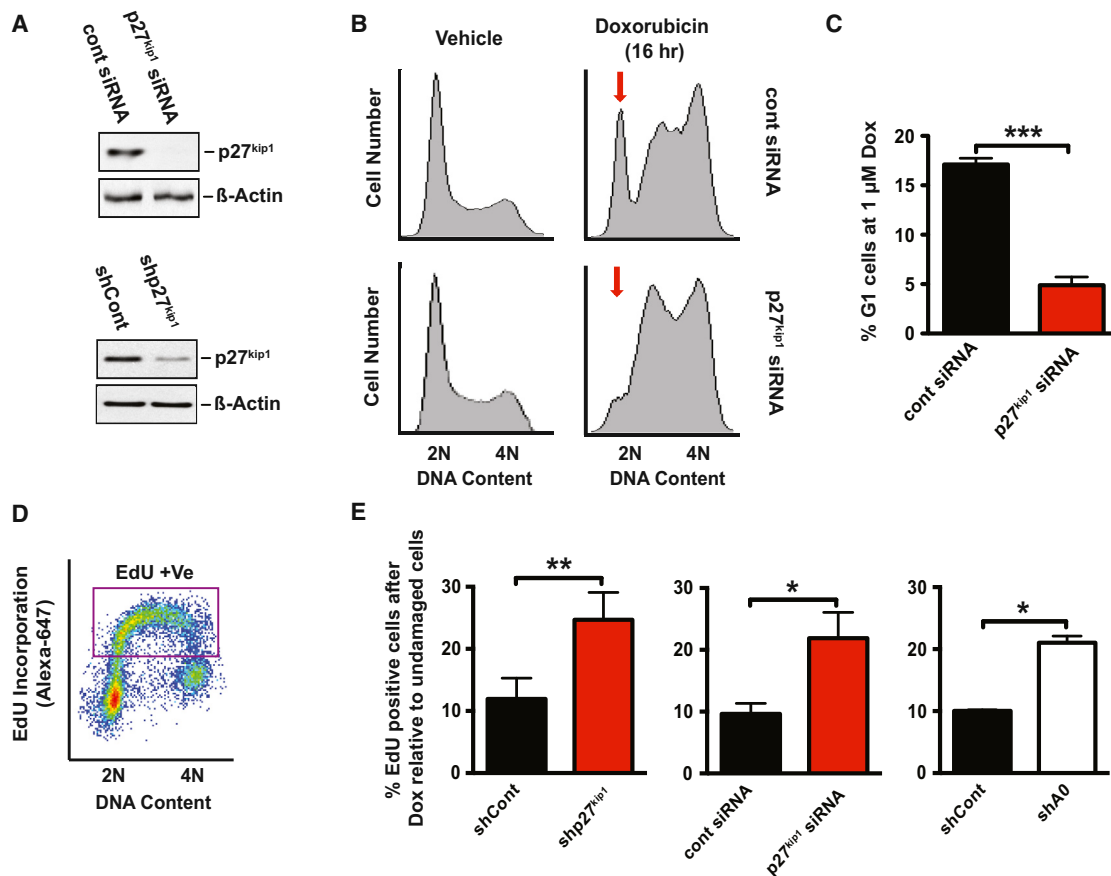


Figure 2. p27^{Kip1} Controls the DNA Damage-Induced G1/S Checkpoint in p53-Deficient Cells

(A) Western blots of H1299 cells transfected with p27^{Kip1}-specific siRNA or infected with a miR-30-based retroviral p27^{Kip1}-specific shRNA (shRNA#1).

(B) Representative flow cytometry profiles of propidium iodide-stained H1299 cells transfected with a control siRNA or a p27^{Kip1}-specific siRNA 16 hr post-doxorubicin treatment. Red arrow indicates loss of the G1 peak in p27^{Kip1}-depleted cells.

(C) Quantification of the percentage of G1-arrested cells from 3 independent experiments performed as in (B). Error bars represent mean \pm SEM, *** p < 0.001.

(D and E) Example of a typical EdU labeling experiment is shown in (D). In (E), loss of p27^{Kip1} causes entry into S-phase despite the presence of DNA damage in a manner and magnitude comparable to that of hnRNPA0 knockdown. Quantified EdU incorporation assays were performed in H1299 cells transfected with a p27^{Kip1}-specific siRNA or transduced with a p27^{Kip1} or hnRNPA0-specific shRNA retrovirus, at 15–16 hr following application of 1 μ M doxorubicin. EdU incorporation values were normalized to those of control undamaged cells treated with vehicle alone (Figures S2B and S2C). Bars represent mean percentage of positive cells relative to vehicle-treated cells (see Figure S2B) \pm SEM, n = 3 experiments. * p < 0.05.

See also Figure S2.

and S1E) suggest that hnRNPA0 protein binds directly to the p27^{Kip1} mRNA via the 3' UTR. Taken together, these observations suggest that the observed upregulation of p27^{Kip1} in response to DNA damage occurs primarily at the post-transcriptional level through increased mRNA stability mediated by hnRNPA0.

p27^{Kip1} Controls the DNA Damage-Induced G1/S Checkpoint in p53-Deficient Cells

p27^{Kip1} is a prototypical CDK inhibitor that binds and inhibits Cyclin A and E/CDK2 and Cyclin D/CDK4 complexes to promote G1 arrest through entry into quiescence (Toyoshima and Hunter, 1994). However, a role for p27^{Kip1} in the establishment of the G1 checkpoint in response to DNA damage has not been well described. This potential role for p27^{Kip1} as a DNA damage-induced G1/S checkpoint regulator would likely be particularly

important in cells with defects or mutations in the p53 pathway because those cells lack the p21(Cip1)-dependent G1/S checkpoint (see Figure 4E), and p27^{Kip1} and p21 perform largely overlapping functions. To test whether this MK2/hnRNPA0/p27^{Kip1} pathway that we have characterized was causally responsible for loss of the G1/S checkpoint in p53-null MK2/hnRNPA0 depleted cells, we knocked down p27^{Kip1} using RNAi (Figure 2A) and monitored the integrity of the G1/S checkpoint by flow cytometry. In control RNAi-treated cells, a substantial fraction of the population (~15%–20%) remains arrested in G1 (Figures 2B, top right, and S2A, top middle) 16 hr after doxorubicin treatment, but this G1 arrest was almost completely ablated upon p27^{Kip1} knockdown (Figures 2B, bottom right, and S2A, bottom middle). Quantification from three independent experiments revealed a near complete loss of G1 cells in the p27^{Kip1} knockdown condition (Figure 2C). We confirmed that the loss of the G1

population in p27^{Kip1}-depleted cells was due to inappropriate progression through the cell cycle, rather than G1-driven cell death, using EdU (5-ethynyl-2'-deoxyuridine) labeling, a thymidine analog that is incorporated into DNA during active synthesis in S-phase (Buck et al., 2008) (Figure 2D). As shown in Figure 2E, DNA damage induced by 1 μ M doxorubicin resulted in a 90% decrease in EdU incorporation when assayed within the 1 hr window between 15 and 16 hr after treatment, relative to undamaged control cells (Figure 2E, black bars; see also Figure S2C) due to implementation of G1/S and intra-S phase checkpoints. However, depletion of p27^{Kip1} with either an siRNA or an shRNA targeting distinct sequences in the p27^{Kip1} mRNA, resulted in a greater than 2-fold increase in EdU incorporation at this time point after damage (Figure 2E, red bars; see also Figure S2C), suggesting that p27^{Kip1}-depleted cells had indeed entered into S-phase due to loss of the G1/S checkpoint (Figure 2B). Importantly, depletion of p27^{Kip1} had no significant effect on EdU incorporation in the absence of DNA damage (Figure S2B). Furthermore, the magnitude of enhanced EdU incorporation following p27^{Kip1} knock-down mirrored that seen with hnRNPA0 knockdown (Figure 2E, white bars; see also Figure S2C), indicating that p27^{Kip1} is the major hnRNPA0-target mRNA controlling the G1/S checkpoint.

MK2-Mediated Phosphorylation of hnRNPA0 in Response to DNA Damage Induces Binding to Its Target RNAs

Because MK2 is an important upstream regulator of hnRNPA0 function through phosphorylation of a single residue, serine 84 (Figure 3A) (Reinhardt et al., 2010; Rousseau et al., 2002), we next examined the role of MK2 on induction of p27^{Kip1} mRNA. As shown in Figures 3B and 3C, depletion of MK2 by RNAi prevented both the DNA damage-induced phosphorylation of serine 84 of hnRNPA0 (Figure 3B) and completely ablated p27^{Kip1} mRNA induction following doxorubicin treatment (Figure 3C). This finding that p27^{Kip1} mRNA is induced in an MK2 and hnRNPA0-dependent manner suggests a direct interaction between hnRNPA0 protein and p27^{Kip1} mRNA (Figures S1D and S1E) that can be modulated by phosphorylation of hnRNPA0 by MK2. To test this, we performed an RNA immunoprecipitation experiment using H1299 cell lines stably expressing HA-tagged WT hnRNPA0 (HA-hnRNPA0-WT), or a mutant version in which the MK2 phosphorylation site was mutated to an alanine (HA-hnRNPA0-S84A) (Figure S3A). As shown in Figure 3D, doxorubicin-induced DNA damage led to an 8-fold increase in the association of p27^{Kip1} mRNA with HA-hnRNPA0-WT and a 14-fold increase in the association of Gadd45 α mRNA (Figure 3D). In contrast, mutation of the MK2 phosphorylation site in hnRNPA0 (Figure 3D, right-most bars) completely eliminated these DNA damage-induced associations. Together with the previous *in vitro* binding experiments (Figures S1D and S1E), these data indicate that p27^{Kip1} mRNA is stabilized in response to DNA damage through a direct interaction with hnRNPA0 in an MK2-regulated manner.

MK2 Phosphorylation of hnRNPA0 Promotes Its Cytoplasmic Accumulation in Response to DNA Damage

MK2 phosphorylation of serine 84 of hnRNPA0 is clearly important for its interaction with its target mRNAs p27^{Kip1} and Gadd45 α (Figure 3D) (Reinhardt et al., 2010), but the molecular

basis has remained elusive. Other members of the hnRNP family of RNA binding proteins shuttle between the nucleus and the cytoplasm under steady-state conditions, but in response to certain extracellular stimuli they can be preferentially retained in one of the two subcellular compartments (Shyu and Wilkinson, 2000). To determine whether hnRNPA0 sub-cellular localization was altered by DNA damage, we subjected H1299 cell lines stably expressing HA-hnRNPA0-WT or HA-hnRNPA0-S84A, to doxorubicin treatment, and examined their localization by subcellular fractionation and by immunofluorescence microscopy of intact cells. In undamaged cells, hnRNPA0 was predominantly nuclear, as assessed by western blotting of fractionated lysates for the HA-tagged protein, lamin A (a nuclear marker) and γ -tubulin (a cytoplasmic marker) (Figure 3E, compare lanes 1 and 3). This was further confirmed by immunofluorescence in whole cells using antibodies against the HA tag (Figure 3F, top row). Doxorubicin-induced DNA damage led to a decrease in the nuclear fraction of hnRNPA0 (Figure 3E, compare lanes 1 and 2) with a concomitant increase in its cytoplasmic abundance (Figure 3E, compare lanes 3 and 4). This was further substantiated by whole cell imaging (Figure 3F, second row, and Figure 3G), indicating that DNA damage induces the cytoplasmic re-localization of hnRNPA0. Strikingly, the non-phosphorylatable HA-hnRNPA0-S84A mutant displayed a similar nuclear-cytoplasmic distribution to HA-hnRNPA0-WT in the basal undamaged state (Figure 3E, lanes 5 and 7), but its localization was entirely unaltered by doxorubicin treatment (Figure 3E, compare lanes 5 and 6; Figures 3F, rows 3 and 4, and 3G). Quantification of the imaging data from multiple experiments revealed an \sim 30% increase in cells with predominantly cytoplasmic HA-hnRNPA0-WT upon doxorubicin treatment that was not observed in the cells expressing the HA-hnRNPA0-S84A phospho-defective form (Figure 3G). Taken together, these biochemical and image-based data indicate that MK2-mediated phosphorylation of hnRNPA0 leads to an increase in its cytoplasmic localization in response to DNA damage where it is well positioned to bind to and stabilize its target mRNAs p27^{Kip1} and Gadd45 α .

Synthetic Lethality between hnRNPA0 Loss and a Defective p53 Pathway in Response to Chemotherapy

Since loss of hnRNPA0 abrogates both the G1 checkpoint through p27^{Kip1} (Figures 1 and 2) and the G2/M checkpoint through Gadd45 α (Reinhardt et al., 2010), thereby reducing the time for DNA repair prior to the next cell cycle transition, we hypothesized that hnRNPA0-depleted cells would be sensitized to killing by DNA-damaging chemotherapy. To test this, cell death was assayed by measuring cleaved caspase 3 in control or hnRNPA0-depleted H1299 cells in response to doxorubicin-induced DNA damage. As shown in Figure 4A, knockdown of hnRNPA0 in human p53-deficient/null H1299 cells resulted in 2-fold more cell death in response to low-dose doxorubicin as compared to control RNAi-treated cells (Figure 4A, black versus white +Dox bars). The effect of hnRNPA0 depletion on cisplatin-induced cell killing was even more pronounced, resulting in a 4-fold increase in death compared to the control vehicle-treated cells (Figure 4B; black versus white +Cis bars). Furthermore, we could recapitulate these findings from human NSCLC cells with two independent shRNAs in a genetically defined murine cell line

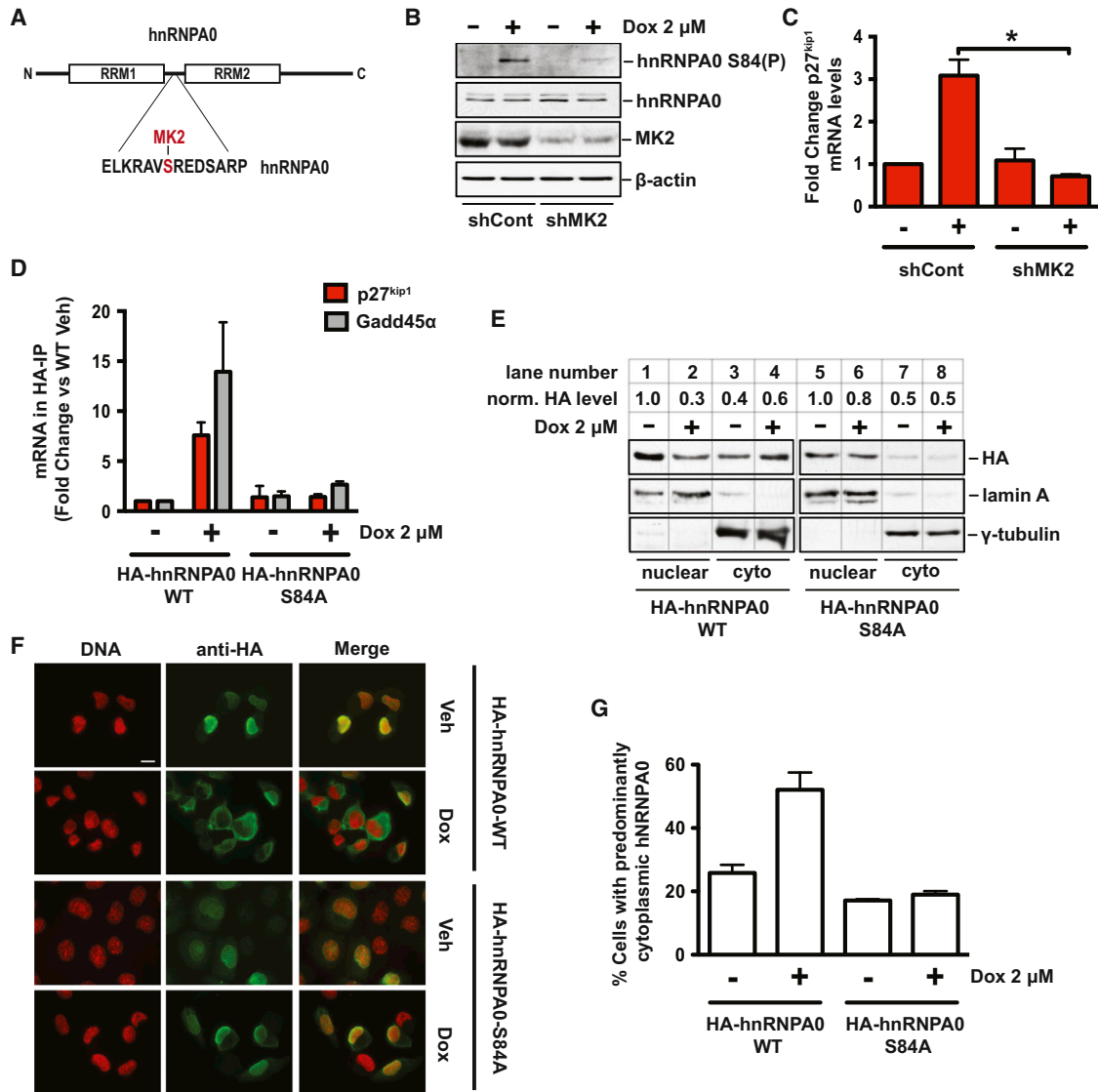


Figure 3. MK2-Mediated Phosphorylation of hnRNPA0 in Response to DNA Damage Induces Binding to Its Target RNAs and Cytoplasmic Localization

(A) Schematic representation of hnRNPA0 domain architecture and sequence surrounding Serine-84 in the linker region between the two RNA recognition motifs (RRMs). The MK2 phosphorylated residue, serine-84, is highlighted in red.

(B) Western blots of H1299 cells transfected with a control shRNA or an MK2-specific shRNA and treated with vehicle or doxorubicin.

(C) qRT-PCR analysis of cells treated as in (B).

(D) Stable H1299 cell lines harboring HA-tagged WT hnRNPA0 or a Ser-84-to-Ala mutant were treated with doxorubicin for 16 hr followed by HA-immunoprecipitation. Co-precipitated RNA was subjected to qRT-PCR for p27^{kip1} and Gadd45 α mRNAs. Data shown as fold-change versus the WT untreated control. Error bars represent mean \pm SEM, n = 2 independent experiments.

(E) Nuclear-cytoplasmic fractionation of H1299 cells following 16 hr doxorubicin treatment.

(F) Immunofluorescence microscopy of H1299 cells fixed 16 hr after 2 μ M doxorubicin treatment. Scale bar represents 5 μ m.

(G) Quantification of hnRNPA0 localization immunofluorescence from two independent experiments, error bars represent mean \pm SEM.

See also Figure S3.

KP7B (Figures 4C and S4A) (Doles et al., 2010) derived from a *K-Ras*^{G12D}; *p53*^{-/-} NSCLC tumor model (Jackson et al., 2005). We further confirmed that our acute measure of cell death in response to DNA-damaging chemotherapy reflected long-term survival of these cells using both colony formation assays (Figure S4B) and fluorescence-labeling based competition assays

(Figures S4C and S4D). These data indicate that loss of hnRNPA0 sensitizes *p53*-null cells to the cytotoxic effects of chemotherapy.

Many human tumors are not entirely *p53*-deficient (i.e., null), but instead have point mutations in critical “hotspot” regions of this prominent tumor suppressor. To determine whether *p53*

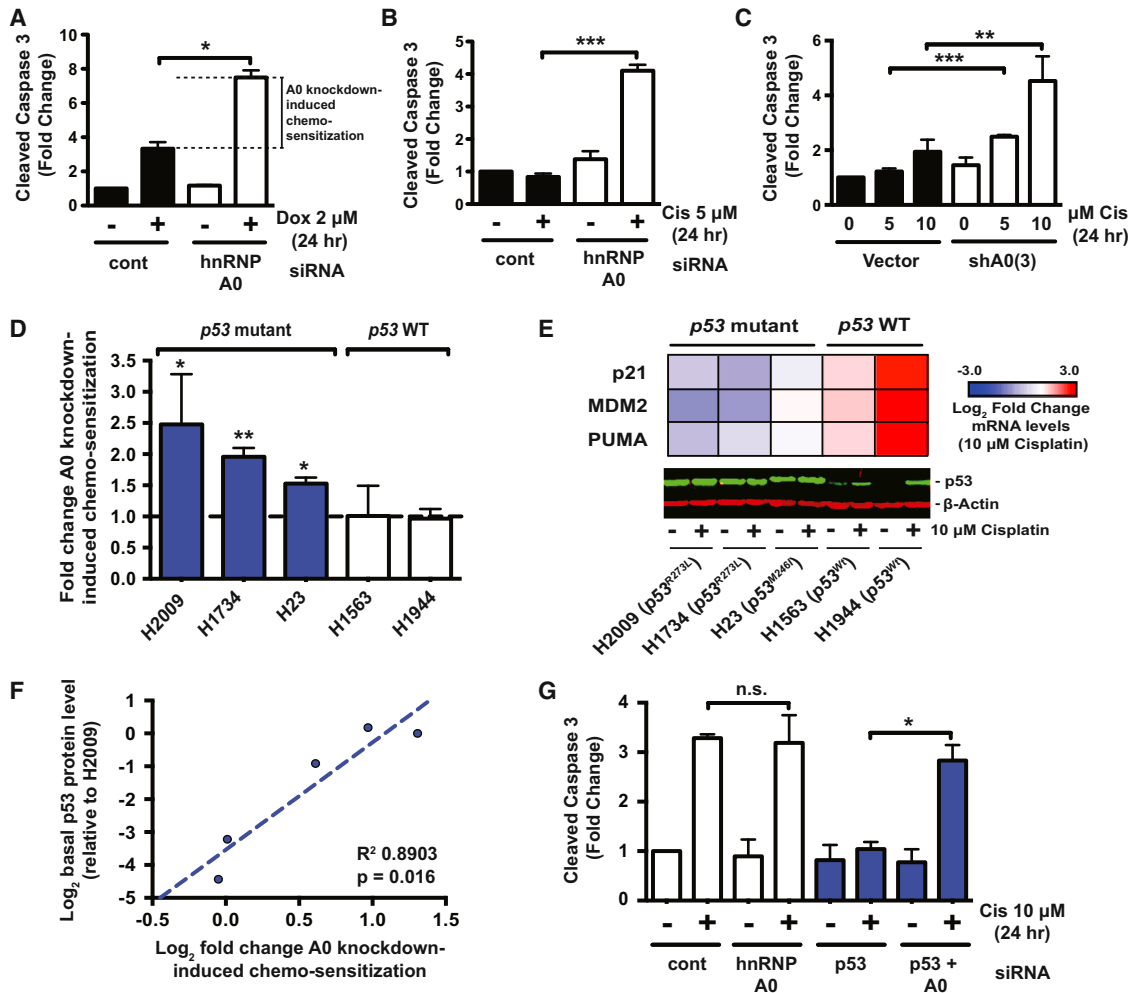


Figure 4. Synthetic Lethality between hnRNPA0 Loss and a Defective p53 Pathway in Response to Chemotherapy

(A and B) H1299 (*p53*-null) cells were transfected with a control or hnRNPA0-specific siRNA and treated with doxorubicin or cisplatin as indicated, followed by western blotting for cleaved caspase 3. Data are represented as fold-change versus control siRNA vehicle-treated cells. Error bars represent mean \pm SEM, $n = 3$ experiments. * $p < 0.05$ ** $p < 0.01$ *** $p < 0.001$.

(C) *K-Ras*^{G12D}; *p53*^{-/-} KPTB murine lung adenocarcinoma cells were transduced with a miR-30 retrovirus expressing an hnRNPA0-specific shRNA and treated as indicated.

(D) A panel of *p53*-mutant and -WT cell lines were transduced or transfected with hnRNPA0-targeting shRNA or siRNA and cell death in response to cisplatin assayed by measuring cleaved caspase 3. Shown is fold change in cell death in cisplatin-treated hnRNPA0-knockdown cells relative to cisplatin-treated control siRNA/shRNA cells. Bars represent mean \pm SEM, $n = 3$ -5. * $p < 0.05$.

(E) Heatmap representation of Log₂ fold change in the mRNA levels of the indicated *p53*-target genes after 16 hr of 10 μ M cisplatin treatment. Lower image is a *p53* western blot of the indicated cell lines treated or not with 10 μ M cisplatin for 16 hr.

(F) *p53* levels from untreated cells from (E) were normalized to beta-actin, Log₂ transformed, and plotted against the Log₂ transformed data from (D). The linear regression and the Pearson R² are shown.

(G) *p53*-WT H1944 cells were transfected with the indicated siRNAs for 48 hr followed by treatment with 10 μ M cisplatin for 24 hr and measurement of cleaved caspase 3. Bars represent mean \pm SEM, $n = 3$. * $p < 0.05$.

See also Figure S4.

status was an important biomarker of chemo-sensitization mediated by hnRNPA0 loss, we knocked down hnRNPA0 by RNAi in a panel of *p53*-mutant and *p53*-WT NSCLC cell lines, treated them with cisplatin, and assayed cell death (Figures 4D and S4F–S4H). As shown in Figure 4D hnRNPA0 knockdown enhanced cisplatin-induced cell death in all *p53*-mutant cell lines to varying degrees, with H2009 and H1734 cells being the most responsive (Figure 4D first two bars). Both of these cell lines express a ho-

mozygous *p53*^{R273L} mutant protein, the most common *p53* mutation found in NSCLC, accounting for >5% of all *p53* mutations (http://p53.free.fr/Database/p53_cancer/p53_Lung.html). Analysis of *p53* target gene expression by qRT-PCR confirmed a largely abrogated *p53* response in the *p53*-mutant cell lines (Figure 4E).

P53 mutations that functionally disable the WT protein often lead to stabilization of *p53* proteins due to loss of a *p53*-driven

MDM2-mediated negative feedback (Olive et al., 2004). Indeed our *p53*-mutant cell lines were characterized by high basal levels of p53 that were not further stabilized upon DNA damage (Figure 4E), in marked contrast to the WT cell lines that expressed low basal levels of p53 that was substantially induced upon DNA damage (Figure 4E). Because not all *p53* mutations disable p53 function equivalently, it has been proposed that higher p53 protein expression can be used as a surrogate marker for more disabling *p53* mutations (Tsao et al., 2007; Yemelyanova et al., 2011). Interestingly, we observed that basal p53 levels (as measured in Figure 4E) were highly correlated with the extent to which hnRNPA0-loss induced chemo-sensitization in our cell line panel (Figure 4F, $R^2 = 0.8903$, $p = 0.016$), suggesting that p53 expression might serve as a generalizable biomarker for the extent to which cells are dependent upon the hnRNPA0 pathway for survival following treatment with DNA-damaging chemotherapy.

Clearly, both *p53*-null and -mutant cells are sensitized to DNA-damaging chemotherapy whereas *p53*-WT cells appear to be unaffected by hnRNPA0 loss. To distinguish whether this synthetic lethal interaction between p53 loss of function and hnRNPA0 depletion was due to chronic adaptive changes in cells with abrogated p53 responses, or an acute effect of p53 loss of function, we then performed combination hnRNPA0/p53 knockdown experiments in *p53*-WT H1944 cells (Figure 4G). Depletion of hnRNPA0 alone had no demonstrable effect on cisplatin-induced cell death in this *p53*-proficient cell line (Figure 4G, compare second and fourth white bars). As expected, p53 knockdown completely abrogated cisplatin-induced cell death (Figure 4G, compare second white bar and second blue bar). Strikingly, combined knockdown of hnRNPA0 on a background of p53 depletion re-sensitized these cells to cisplatin-induced cell death (Figures 4G, compare second and fourth blue bars, and S4H). Similar results were obtained with doxorubicin treatment in A549 cells, a second *p53*-WT cell line, upon single and combined hnRNPA0/p53 knock-down (Figure S4I). These data suggest that targeting of hnRNPA0 can sensitize cells that have acutely lost p53 function to DNA-damaging chemotherapy.

To address the importance of MK2 phosphorylation of hnRNPA0 in mediating cisplatin resistance, we performed knockdown-rescue experiments with WT and mutant hnRNPA0 in KP7B cells (Figure S4J). Endogenous hnRNPA0 was knocked-down with a retroviral shRNA targeting the 3' UTR followed by reconstitution with either HA-hnRNPA0-WT or HA-hnRNPA0-S84A cDNA of human origin (Figure S4J, upper image; note mobility shift due to the 2× HA-tag). These cells were then treated with cisplatin and assayed for cell death (Figure S4J, middle). Knockdown of hnRNPA0 increased cell death in response to cisplatin (Figure S4J, bottom; compare second black bar and second white bar), whereas re-expression of HA-hnRNPA0-WT completely abrogated this effect (Figure S4J, bottom; compare second white bar to fourth white bar). In stark contrast, re-expression of HA-hnRNPA0-S84A failed to rescue the hnRNPA0 knockdown phenotype (Figure S4J, bottom; compare second white bar and sixth white bar). These data suggest that phosphorylation of hnRNPA0 is not only required for its interaction with target mRNAs, but also required for cells to resist killing by chemotherapy, potentially due to a requirement for damage-induced hnRNPA0 cytoplasmic localization (Figure 3).

Reduced hnRNPA0 Activity Promotes Cisplatin Efficacy In Vivo in a Murine *p53*-Deficient NSCLC Model

To determine whether hnRNPA0 promotes resistance of established lung tumors to cisplatin-based chemotherapy in vivo, we took advantage of a transplantable model of NSCLC (Doles et al., 2010; Morandell et al., 2013). In this model, KP7B cells are transplanted in syngeneic, immune-competent recipient mice (Figure 5A) (Doles et al., 2010). The advantages of this model over a traditional xenograft approach are 3-fold: First, tumors arising in recipient mice are pathologically and molecularly indistinguishable from the tumors from which they were derived (Doles et al., 2010), which are themselves strikingly similar to their human counterparts (Jackson et al., 2005; Sweet-Cordero et al., 2004). Second, the cells give rise to tumors in the correct anatomical location in the presence of a fully functional host immune system. Lastly, and most importantly for our studies, this model is highly tractable and allows genetic manipulation of proteins of interest prior to transplantation.

We generated stable KP7B cell lines by introduction of an hnRNPA0-specific shRNA that efficiently knocked down its intended target (Figure S5A), along with a retrovirus expressing luciferase to facilitate imaging of response to therapy (Figure 5A). These cell lines were then transplanted into multiple syngeneic recipient mice, and tumors were allowed to form until strong bioluminescence was observed in the lungs of all animals (16 days post-transplantation) to assess therapeutic response in established tumors. Although no significant difference in bioluminescence was observed between control and hnRNPA0-depleted tumors in the absence of DNA-damaging chemotherapy (Figures 5B and 5C; Figure S5B, pre-treatment condition), upon treatment with cisplatin, control tumors continued to grow rapidly but growth of hnRNPA0-depleted tumors was markedly suppressed (Figures 5B and 5C). MicroCT imaging of a second cohort of animals treated with a single high dose of cisplatin (10 mg/kg) confirmed the superior response of hnRNPA0-depleted tumors to chemotherapy (Figures S5B–S5D). Consistent with the short term tumor response data, mice transplanted with hnRNPA0-proficient cells obtained no significant survival benefit from cisplatin treatment (Figure 5D, compare red and blue lines, $p = 0.52$) indicating that tumors in this model are entirely recalcitrant to cisplatin-based chemotherapy (Doles et al., 2010). In contrast, animals transplanted with hnRNPA0-depleted tumors displayed a significant survival benefit upon cisplatin treatment (Figure 5E, compare red and blue lines, $p < 0.0001$) indicating that the acute tumor growth effect we observed in response to therapy (Figures 5B and 5C) directly translated into an extension of lifespan in this murine NSCLC model (Figures 5D and 5E). Taken together, these data indicate that the presence of hnRNPA0 promotes resistance of established lung tumors to cisplatin-based chemotherapy in vivo.

hnRNPA0 Promotes Resistance to Chemotherapy through Stabilization of p27^{Kip1} and Gadd45 α mRNAs

Our data demonstrate that in response to DNA-damaging chemotherapy, MK2-mediated phosphorylation of hnRNPA0 stabilizes the mRNAs of p27^{Kip1} and Gadd45 α to control the G1/S and G2/M checkpoints, respectively (Figure 6A). However, the relative contributions provided by either of these two target

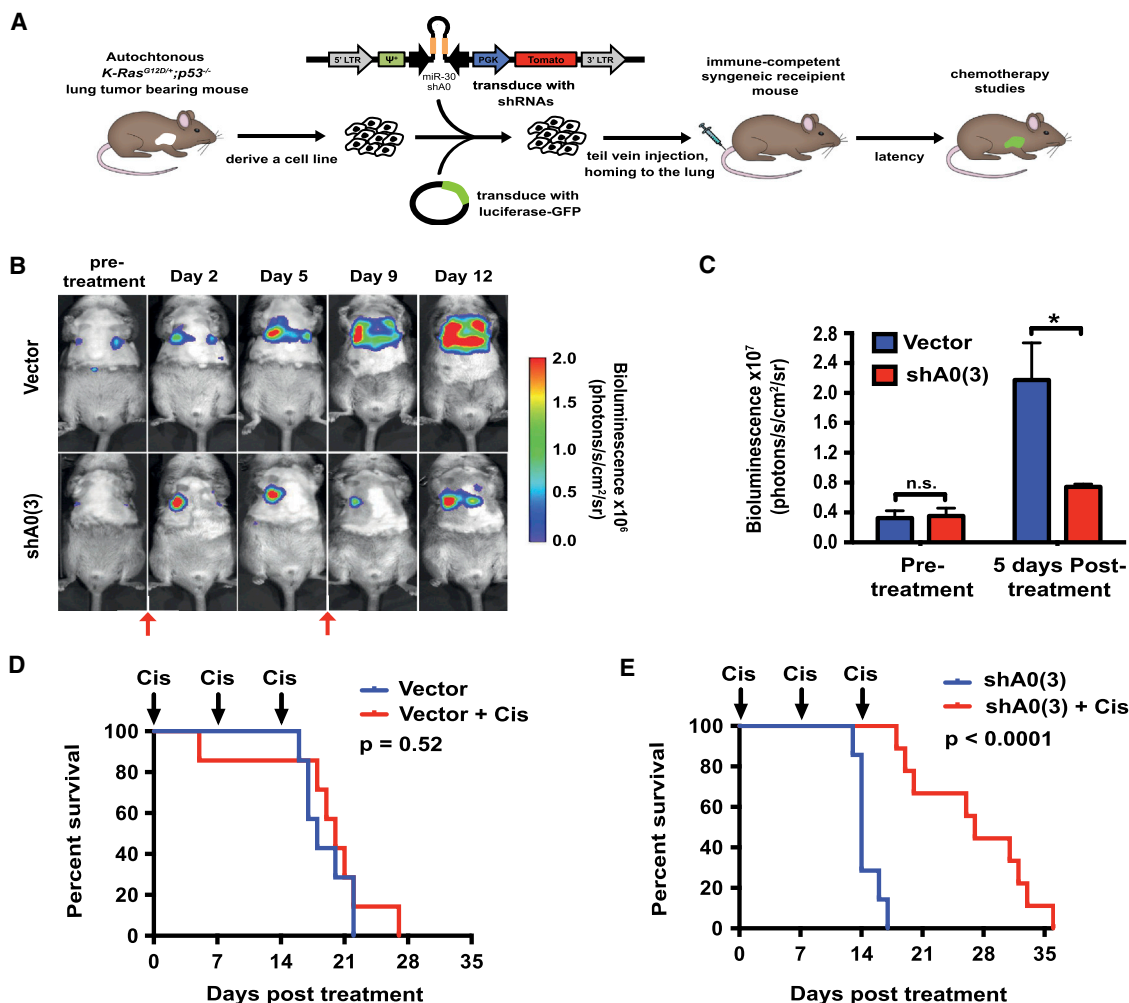


Figure 5. Decreased hnRNPA0 Activity Promotes Cisplatin Efficacy against p53-Defective NSCLC In Vivo

(A) Schematic representation of the transplatable NSCLC model.

(B) Representative bio-luminescence images before and after cisplatin treatment on Days 0 and 7. Red arrows indicate timing of cisplatin dosing.

(C) Quantification of lung bio-luminescence pre-treatment and 5 days post-cisplatin treatment. Error bars represent mean \pm SEM, three to four animals per condition, * $p < 0.05$.

(D) Post-treatment Kaplan-Meier survival analysis of control tumor-bearing mice with or without cisplatin treatment, as indicated. (Vector $n = 7$, vector + Cis $n = 7$).

(E) Post-treatment Kaplan-Meier survival analysis of shA0 tumor-bearing mice with or without cisplatin treatment, as indicated. (shA0(3) $n = 7$, shA0(3) + Cis $n = 9$).

p values in (D) and (E) were calculated using the log-rank test.

See also Figure S5.

mRNAs to the overall enhanced chemosensitivity of hnRNPA0 knockdown cells/tumors (Figures 4 and 5) are unknown. To determine this, we depleted p53-null H1299 cells of either p27^{Kip1} alone, Gadd45 α alone, or both RNAs simultaneously. The isolated or combined knockdown of p27^{Kip1} and Gadd45 α had no significant effect on untreated cells, indicating that loss of these two proteins is not acutely toxic to cells in the absence of DNA damage (Figures 6B, S6A, and S6B). Knockdown of either of these hnRNPA0-target mRNAs individually had no effect on cell death in response to cisplatin (Figure 6B, red and blue bars compared to the black bars) or doxorubicin (Figure S6B). Strikingly, however, co-depletion of both hnRNPA0-target mRNAs resulted in a markedly enhanced amount of cell death, and fully recapitulated the effect of hnRNPA0 knockdown

on response to cisplatin (Figure 6B, compare white bars and purple bars) and doxorubicin (Figure S6B). Taken together, these data indicate that MK2/hnRNPA0 promotes the resistance of p53-defective cells to chemotherapy by the combined action of stabilizing both p27^{Kip1} and Gadd45 α mRNAs to control the G1/S and G2/M checkpoints, respectively.

Reduced Levels of hnRNPA0-Target mRNAs Correlate with Favorable Response to Adjuvant Chemotherapy in Patients with NSCLC

The observation that the MK2/hnRNPA0 pathway promotes resistance to chemotherapy in NSCLC models through the coordinate post-transcriptional control of the p27^{Kip1} and Gadd45 α -regulated DNA damage G1/S and G2/M checkpoints

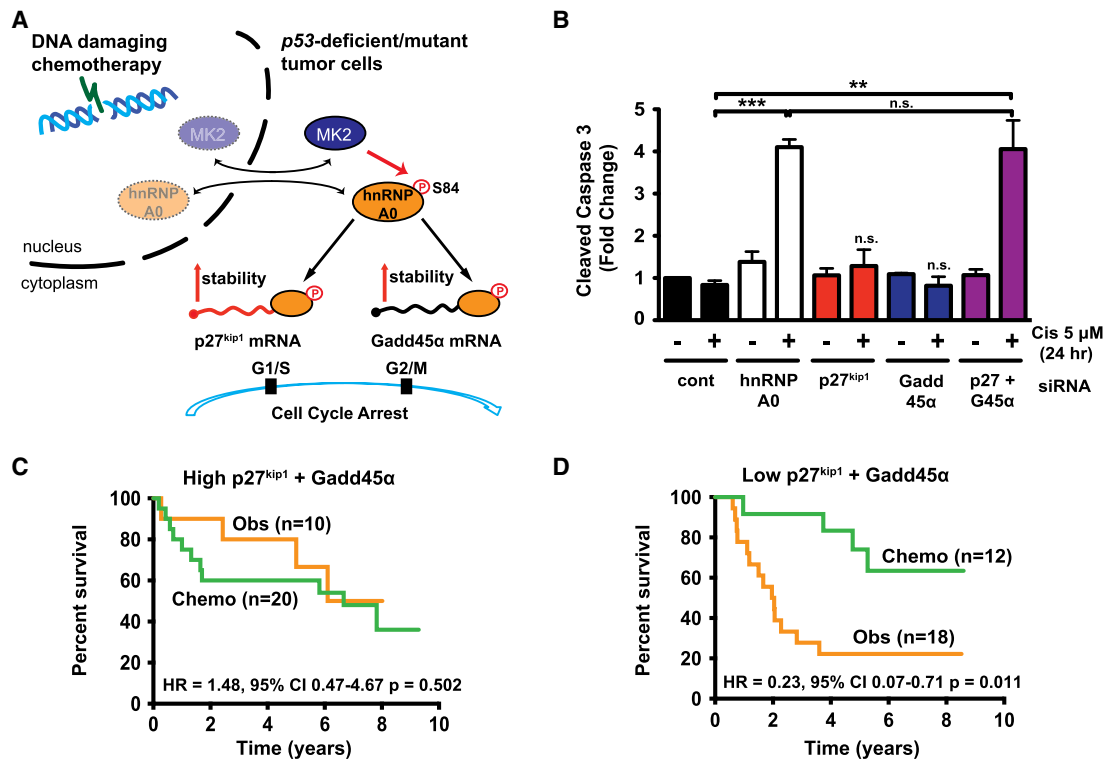


Figure 6. hnRNPA0 Promotes Resistance to Chemotherapy through p27^{Kip1} and Gadd45 α

(A) Model depicting the role of MK2, hnRNPA0, p27^{Kip1}, and Gadd45 α in the DNA damage response, limiting the efficacy of anti-cancer chemotherapy.

(B) H1299 (p53-null) cells were transfected with the indicated siRNAs and analyzed as in Figure 4. Error bars represent mean \pm SEM, n = 3 experiments. **p < 0.01, ***p < 0.001, n.s. = not significant. Control siRNA and A0 siRNA data from Figure 4B are shown again here for comparison.

(C and D) Patients with stage 2 disease from the JBR.10 lung cancer adjuvant chemotherapy trial were clustered into two groups based on expression of both p27^{Kip1} and Gadd45 α . Patients in this trial were either observed (Obs, orange line) or treated with cisplatin/vinorelbine-based chemotherapy (Chemo, green line). Kaplan-Meier analysis based on expression of MK2/hnRNPA0-target mRNAs demonstrates that only those patients with low levels of these mRNAs benefit significantly from adjuvant chemotherapy. The p values were calculated using the log-rank test.

See also Figure S6.

suggests that human tumors with low levels of activity through this pathway, either by means of natural heterogeneity or pharmacological intervention, might be more likely to respond to cisplatin-based chemotherapy. To test this, we made use of data from the NCIC CTG JBR10 clinical trial in which patients with stage 1B or 2 NSCLC underwent surgical resection and were then either observed or given cisplatin/vinorelbine adjuvant chemotherapy (Winton et al., 2005). This dataset was selected for analysis for several reasons. First, banked snap-frozen tumors from a subset of patients were subjected to gene expression profiling prior to therapy, thus facilitating identification of genetic determinants of therapeutic response (Zhu et al., 2010). Second, this trial had a control/observation arm thus allowing for factors that regulate response to therapy (predictive markers) to be differentiated from those that affect tumor growth per se (prognostic markers). Unsupervised clustering on p27^{Kip1} and Gadd45 α expression was used as a surrogate for assessing activity through the MK2/hnRNPA0 pathway and two distinctive clusters were identified (Figure S6C): one cluster with high expression of p27^{Kip1} and Gadd45 α and the other with low expression. We focused our analysis on patients with stage 2 NSCLC (Table 1) because adjuvant chemotherapy has been

shown to be beneficial mainly in this subset of patients with early stage disease (Winton et al., 2005). As shown in Figure 6C, patients with high expression of p27^{Kip1} and Gadd45 α did not benefit from adjuvant chemotherapy (Figure 6C, compare orange and green lines, HR 1.48, 95% CI 0.47–4.67, p = 0.502). Whereas, patients with low levels of these hnRNPA0-target mRNAs received significant benefit from adjuvant chemotherapy (Figure 6D, compare orange and green lines, HR 0.23 95% CI 0.07–0.71 p = 0.011). Importantly, patients in the observation arm of the trial whose tumors express low levels of p27^{Kip1} and Gadd45 α appeared to show the poorest survival of all groups analyzed (Figure 6D, orange line) similar to mice harboring hnRNPA0-depleted tumors (Figures 5D and 5E, compare blue line in 5D to the blue line in 5E; p = 0.0023). Moreover, only consideration of both p27^{Kip1} and Gadd45 α expression together, but neither alone, had a significant association with therapeutic response (Figure S6D). Because our data from a panel of NSCLC cell lines indicated that high basal p53 protein levels correlated with superior response to hnRNPA0 knockdown-induced chemosensitization (Figures 4D–4F), we further stratified patients based upon p53 immuno-histochemistry status: p53 IHC positive/putatively mutant and p53 IHC

Table 1. Association of p27^{Kip1}/Gadd45 α Expression with Clinical Factors in Stage 2 NSCLC

Parameter	Expression of p27 and GADD45 α			p Value
		High (% , n = 30)	Low (% , n = 30)	
Histology	ADC	16 (55.2)	13 (44.8)	0.725
	SQCC	12 (44.4)	15 (55.6)	
	LCUC	2 (50.0)	2 (50.0)	
Chemotherapy	OBS	18 (64.3)	10 (35.7)	0.038
	ACT	12 (37.5)	20 (62.5)	
Age (yr)	<65	26 (49.1)	27 (50.9)	0.688
	\geq 65	4 (57.1)	3 (42.9)	
Sex	male	24 (53.3)	21 (46.7)	0.371
	female	6 (40.0)	9 (60.0)	
P53 IHC ^a	negative	11 (44.0)	14 (56.0)	0.571
	positive	14 (51.9)	13 (48.1)	
	unknown	5 (62.5)	3 (37.5)	

^aNegative is used as a surrogate of wild type p53, positive as a surrogate of p53 with missense mutation.

negative/putatively WT (Tsao et al., 2007). Although the number of patients is very small, the data suggest that patients whose tumors express low levels of p27^{Kip1} and Gadd45 α , and additionally have stabilizing p53 mutations, benefit most from adjuvant cisplatin-based chemotherapy (Figures S6E and S6F). Taken together, these murine (Figure 5) and human clinical data (Figures 6 and S6) indicate that hnRNPA0 promotes resistance to chemotherapy in p53-mutant NSCLC through p27^{Kip1} and Gadd45 α (Figure 6A).

Mutual Exclusivity of the p53 and MK2/hnRNPA0 Pathways Is Ensured by p53/p21-Mediated Suppression of hnRNPA0

To ascertain the molecular basis for the p53 context-dependence of hnRNPA0 for DNA damage tolerance, we next investigated whether there is a regulatory relationship between p53 and hnRNPA0. We noted that when p53-proficient cells were treated with doxorubicin, a marked suppression of hnRNPA0 protein levels was observed (Figure 7A, compare lanes 1 and 2 and first two black bars), that was not seen in p53-null cells (see Figure 1E). To examine whether this reduction in hnRNPA0 required p53, we knocked down p53 with siRNA, treated the cells with doxorubicin, and measured hnRNPA0 protein levels. The pronounced decrease in hnRNPA0 following DNA damage that we observed previously was largely ablated upon p53 knockdown (Figure 7A) suggesting that p53 or its downstream effectors actively suppresses hnRNPA0. Conversely, activation of p53 even in the absence of DNA damage was sufficient to suppress hnRNPA0. In these experiments treatment of A549 cells with the MDM2 inhibitor Nutlin 3a to upregulate p53 resulted in downregulation of hnRNPA0 protein and mRNA in control siRNA-transfected cells (Figure 7B, left and right lower images, black bars), but not in p53-depleted cells (Figure 7B, red bars). These findings suggest that the drop in hnRNPA0 protein levels is likely a consequence of decreased mRNA levels, either due to decreased transcription, or to post-transcriptional destabilization of the hnRNPA0 mRNA.

Because many RNA-binding proteins are auto-regulated or regulated by other RNA-BPs at the post-transcriptional level, and the hnRNPA0 3' UTR is long and highly conserved (Figure S7A), we first examined whether hnRNPA0 mRNA was destabilized upon p53 activation. To test this, we measured hnRNPA0 mRNA stability in Nutlin 3a-treated cells in the same manner as we had assessed p27^{Kip1} mRNA stability in response to doxorubicin (Figure 1G). As shown in Figure 7C, the half-life of hnRNPA0 mRNA dropped from \sim 16 hr in vehicle-treated cells to \sim 6 hr following p53 activation with Nutlin 3a. Moreover, half-life estimates averaged from multiple experiments revealed an \sim 50% decrease in hnRNPA0 mRNA half-life upon p53 activation (Figure 7D), closely mirroring the drop seen in total hnRNPA0 mRNA levels (Figure 7B, right, black bars). Because p21 is the primary effector of p53-mediated G1/S checkpoint control, we next asked whether suppression of the hnRNPA0 successor pathway was p21-dependent. We knocked down p21 using siRNA in A549 cells, treated them with Nutlin 3a to activate p53 (Figure 7E, left) and measured hnRNPA0 protein and mRNA levels. Indeed, the repression of hnRNPA0 mRNA (Figure 7E, right) and hnRNPA0 protein (Figure S7B) was largely ablated by depletion of p21. Although the precise molecular basis for this p21-dependent hnRNPA0 mRNA destabilization remains to be determined, these findings clearly point to an important role for p21 induction in suppression of hnRNPA0 expression. These data suggest that rather than functioning in parallel pathways, the primary p53/p21 and the successor MK2/hnRNPA0 pathways of cell cycle checkpoint control are mutually exclusive, and that this is ensured by suppression of the successor pathway at the level of hnRNPA0 mRNA destabilization (Figure 7F).

DISCUSSION

Post-transcriptional control of gene expression is becoming increasingly appreciated as a target of the DDR. Several unbiased screens have implicated RNA binding proteins (RNA-BPs) as one of the most enriched classes of genes involved in activating and modulating the DDR (Beli et al., 2012; Matsuoka et al., 2007; Paulsen et al., 2009; Reinhardt et al., 2010). To date, however, there are few examples of RNA-BPs that have been implicated as functionally important in the execution of specific cellular decisions in response to DNA damage, or had their relevant target RNAs interrogated in this regard (Abdelmohsen et al., 2007). Here we have shown that the RNA-BP hnRNPA0 is a major substrate of the checkpoint kinase MK2, and that it enforces cell cycle arrest and promotes resistance to DNA-damaging chemotherapy through two distinct target mRNAs that respectively control the G1/S and G2/M DNA damage checkpoints in cultured cells and in vivo. These findings indicate that in addition to modulating the DDR itself, RNA-BPs are intimately involved in critical life and death decisions. More broadly, recent advances in the high-throughput identification of RNA-protein interactions, such as high throughput sequencing crosslink immunoprecipitation (HITS-CLIP) (Darnell, 2010), should help to elucidate the role of other RNA-BPs identified in recent screening approaches and may shed light on the breadth and extent of post-transcriptional control of gene expression in the context of the DDR.

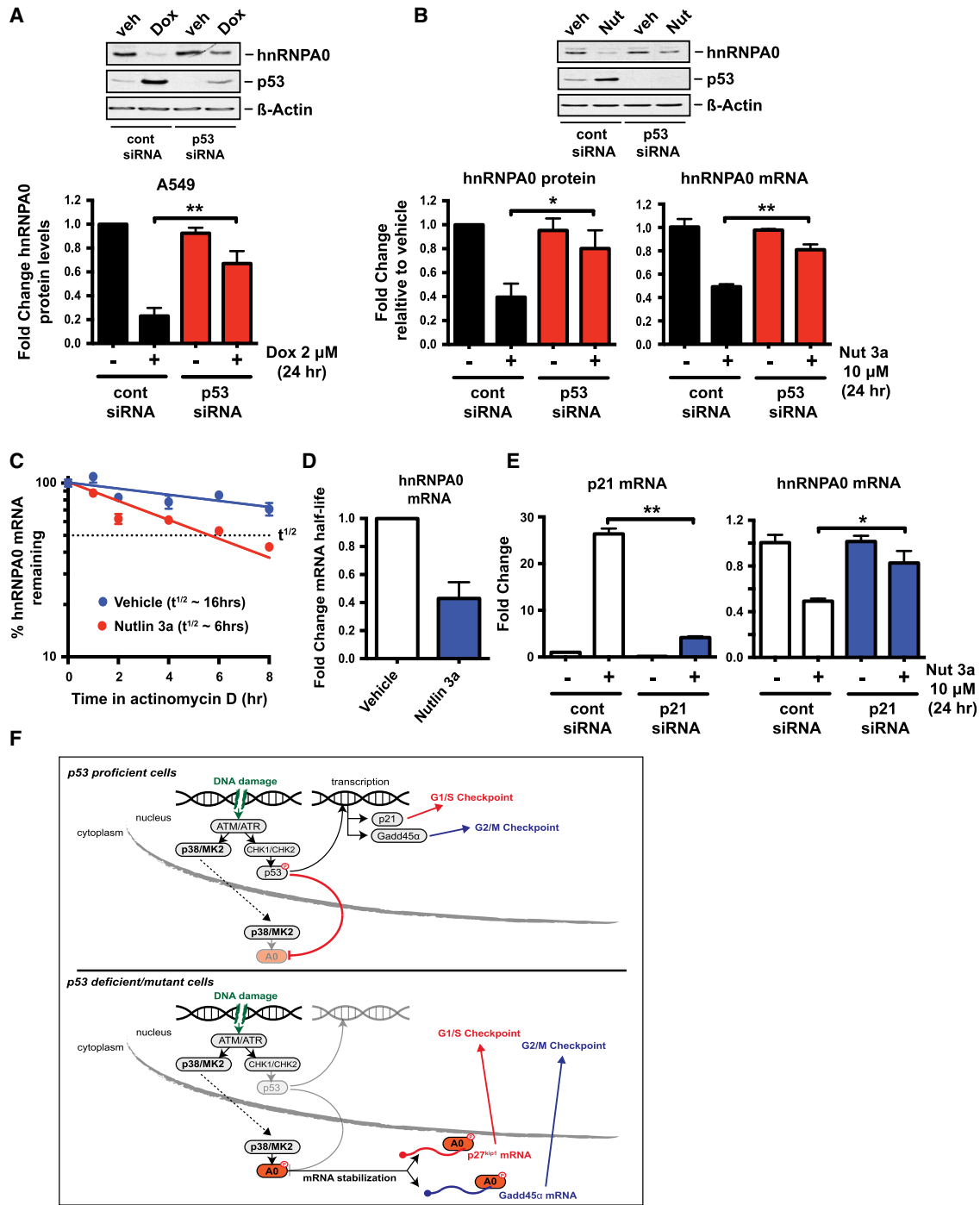


Figure 7. The Primary p53/p21 Axis Actively Suppresses the Successor hnRNPA0 Pathway

(A) p53-WT A549 cells were transfected with a control siRNA or a p53-targeting siRNA for 48 hr, followed by treatment with 2 μM doxorubicin for 24 hr. hnRNPA0 protein expression was measured by western blotting. Data are plotted as fold-change in hnRNPA0 protein (normalized to actin) relative to vehicle-treated control siRNA transfected cells, bars represent mean ± SEM, n = 3 experiments. **p < 0.01.

(B) p53-WT A549 cells were transfected with siRNAs as in (A), then treated with 10 μM MDM-2 inhibitor/p53 activator Nutlin 3a for 24 hr. Left: data are plotted as fold-change in hnRNPA0 protein (normalized to actin) relative to vehicle-treated control siRNA transfected cells, bars represent mean ± SEM, n = 4 experiments. *p < 0.05. Right: data are plotted as fold-change in hnRNPA0 mRNA relative to vehicle-treated control siRNA transfected cells, bars represent mean ± SEM, n = 3 experiments. **p < 0.01.

(C) A549 cells were treated as in (B) except that at 24 hr actinomycin D was added to the culture medium and time points taken for RNA analysis by qRT-PCR. Data represent percent remaining hnRNPA0 mRNA for each condition relative to the 24 hr time point where actinomycin was added.

(legend continued on next page)

Our work demonstrates that hnRNPA0 regulates p27^{Kip1} expression in a context-specific manner in response to DNA-damaging chemotherapy and complements a growing body of literature documenting the critical contribution of post-transcriptional control by multiple regulators (e.g., miR-221, DND1 and Pumilio) to p27^{Kip1} expression (Kedde et al., 2007, 2010). The binding of hnRNPA0 to p27^{Kip1} mRNA appears to occur via the 3' UTR but in a region that is distinct from that of miR-221, DND1 or Pumilio (Kedde et al., 2007, 2010). Together these data indicate that the p27^{Kip1} 3' UTR acts as a platform for different post-transcriptional regulators dependent upon the extracellular cues (e.g., growth factors, DNA damage, etc.) and genetic context (e.g., p53 mutation) in which a specific cell exists.

MK2 activation of cell cycle checkpoints in p53-compromised cells promotes resistance to doxorubicin or cisplatin-based chemotherapy, raising the possibility that targeting this pathway in human tumors may preferentially kill p53-mutant tumor cells while sparing p53-WT normal cells (Morandell et al., 2013; Reinhardt et al., 2007). MK2 controls the G2/M checkpoint by regulating the activity of the RNA-BP hnRNPA0 and causing stabilization of Gadd45 α mRNA (Reinhardt et al., 2010). Here we have shown that, in addition to regulation of the G2/M checkpoint, hnRNPA0 also enforces a G1/S checkpoint through stabilization of p27^{Kip1} mRNA. Traditionally p27^{Kip1} is regarded as the major CDK inhibitor that induces G1 arrest upon contact inhibition or during terminal differentiation (Hsieh et al., 2000; Polyak et al., 1994) but a role for p27^{Kip1} in control of the DNA damage checkpoints has largely been overlooked with two notable exceptions (Cuadrado et al., 2009; Lontos et al., 2010). Our data clearly implicate p27^{Kip1} as the major controller of the G1/S checkpoint following DNA damage in p53-null cells. Interestingly, a previous report implicated p27^{Kip1} in long-term maintenance of cell cycle arrest in p53-WT A549 cells after long-term exposure to doxorubicin (Cuadrado et al., 2009). In that study p27^{Kip1} was only important for controlling the G1/S checkpoint once the initial wave of p53-p21 activity had diminished (Cuadrado et al., 2009). In agreement with these observations, we show that in those same p53-WT A549 cells acute (24 hr), activation of p53 by doxorubicin or MDM2 inhibition suffices to downregulate hnRNPA0 in a p53/p21-dependent manner. These data support a mutual exclusivity model where p27^{Kip1} control of the G1/S checkpoint only becomes essential in cells that do not have an active p53-p21 pathway and thus fail to suppress hnRNPA0 (Figure 7F). Interestingly, Gadd45 α is a transcriptional target of p53 in response to DNA damage, but in p53-null cells is induced by the MK2/hnRNPA0-dependent stabilization of its mRNA. Therefore, Gadd45 α control of the G2/M checkpoint is functionally maintained in the absence of p53 by a switch from transcriptional to post-transcriptional control (Figure 7F). Together these data indicate that hnRNPA0 is the “successor” to p53 for checkpoint control in response to DNA-damaging chemotherapy and that a

mechanistic switch from transcriptional control of p21 and Gadd45 α to post-transcriptional control of p27^{Kip1} and Gadd45 α enforces the G1/S and G2/M checkpoints and drives chemoresistance (Figure 7F).

Intrinsic drug resistance is a major obstacle to the successful treatment of human malignancies. Some patients receive significant benefit from cytotoxic DNA-damaging chemotherapy but identifying these patients a priori is a significant challenge (Kelland, 2007). Here, we have shown that p53-null/mutant NSCLCs rely on an MK2/hnRNPA0/p27^{Kip1}/Gadd45 α pathway to promote cell cycle arrest and resist killing by chemotherapy. In light of our findings in tumor cell lines and animal models, we investigated whether the status of this pathway correlated with therapeutic response in patients with NSCLC. Consistent with our experimental data, we observed that patients with stage 2 NSCLC with low levels of hnRNPA0-target mRNAs received significant benefit from adjuvant chemotherapy after surgical resection that was exacerbated still further when analyzing patients with p53-mutant tumors, whereas those with high levels of MK2/hnRNPA0-target mRNAs did not. Although our findings in this well-annotated small patient cohort will require independent large scale verification, our data suggest that the use of p27^{Kip1} and Gadd45 α mRNA levels in combination with p53 IHC as predictive biomarkers could identify a subset of patients at diagnosis who are most likely to benefit from platinum-based chemotherapy. Our data therefore highlight a critically important unifying role for the cytoplasmic MK2/hnRNPA0 p53-successor pathway in dictating tumor response to therapy in NSCLC through post-transcriptional control of two distinct cell cycle checkpoints (Figure 7F).

EXPERIMENTAL PROCEDURES

RNA-IP and qRT-PCR

RNA-IPs were performed as described previously (Reinhardt et al., 2010) with the addition of 4-thiouridine (4SU) labeling prior to drug treatment. Briefly, H1299 cells expressing HA-hnRNPA0 were treated with 100 mM 4SU for 24 hr, followed by treatment with 2 μ M doxorubicin for 16 hr. At the end of doxorubicin treatment, cells were washed once in ice-cold PBS and cross-linked at 365 nm as described (Hafner et al., 2010). Cells were then scraped in ice-cold PBS and RNA-IP performed as described previously (Keene et al., 2006; Reinhardt et al., 2010) using HA-agarose beads (Sigma-Aldrich). For qRT-PCR analysis, RNA was extracted using TRIzol reagent (Ambion) according to the manufacturer's instructions and 1 μ g of total RNA was used for reverse transcription using the superscript III first-strand synthesis kit (Invitrogen) and oligo-dT priming as per the manufacturer's instructions. For qPCR, cDNA was amplified using SYBR green PCR mastermix (Applied Biosystems) according to the manufacturer's cycling conditions for 40 cycles on a Bio-Rad C1000 Thermal Cycler. Data were analyzed using the delta-delta Ct method as described previously (Cannell et al., 2010) and plotted as fold change versus control.

Murine NSCLC Transplant Model

A total of 50,000 KP7B cells, labeled with GFP-luciferase, were transplanted into 10- to 12-week-old syngeneic C57BL6/Jx129-JAE male

(D) Slopes of the lines from three independent experiments performed as in (C) were calculated and used to determine the fold change in mRNA half-life upon p53 activation. Bars represent mean \pm SEM.

(E) A549 cells were transfected with a control siRNA or a p21-targeting siRNA for 48 hr, followed by treatment with 10 μ M Nutlin 3a for 24 hr. p21 and hnRNPA0 mRNA expression was measured by qRT-PCR. Data are plotted as fold-change in mRNA levels relative to vehicle-treated control siRNA transfected cells, bars represent mean \pm SEM, n = 3 experiments. *p < 0.05, **p < 0.01.

(F) Model representation of the interplay between the p53 and MK2/hnRNPA0 pathways in response to DNA-damaging chemotherapy. See also Figure S7.

recipient mice 6 hr after 5 Gy whole-body irradiation as described previously (Doles et al., 2010). Tumors were allowed to form for approximately 2 weeks and tumor growth was measured by microCT imaging on a eXplore CT120-whole mouse MicroCT (GE Healthcare) (45 μm resolution, 80 kV, with 450 μA current) as described previously (Doles et al., 2010) or bio-luminescent imaging on a IVIS Spectrum-bioluminescent and fluorescent imaging system (Xenogen). For all imaging procedures, animals were pre-anesthetized with isoflourane. For drug treatments, cisplatin was dissolved in saline and injected intraperitoneally at 10 mg/kg for single high-dose treatment, or with 7 mg/kg once weekly for 3 weeks for low-dose treatment. Mice were killed when they were moribund or when they had lost 20% of their initial body weight, whichever occurred sooner, according to MIT Committee on Animal Care guidelines. All mouse studies were approved by the MIT Institutional Committee for Animal Care, and conducted in compliance with the Animal Welfare Act Regulations and other federal statutes relating to animals and experiments involving animals and adheres to the principles set forth in the Guide for the Care and Use of Laboratory Animals, National Research Council, 1996 (Institutional Animal Welfare Assurance no. A-3125-01).

Retrospective Analysis of p27^{Kip1} and Gadd45 α mRNA Expression and Therapeutic Response in NSCLC

This study used human tissues from a snap-frozen lung tumor bank that was established at the Princess Margaret Hospital and Toronto General Hospital in 1996, after approval by the Research Ethics Board of the University Health Network. Patients' demographic and clinical follow-up information was also obtained after Research Ethics Board approval for chart reviews. Expression of p27^{Kip1} and Gadd45 α mRNAs in 133 NSCLC samples were profiled by using Affymetrix U133A (Zhu et al., 2010) represented by probe set 209112_at and 203725_at, respectively. Two clusters were identified based on the expression of p27^{Kip1} and Gadd45 α using hierarchical clustering (Sturn et al., 2002). The two clusters were defined as low and high expressed groups based on the expression of these two genes (Figure S6C). For survival analysis, lung cancer specific survival was used as the survival endpoint and Cox proportional hazards regression (SAS v9.3, SAS Institute) was used to estimate the hazard ratio and test the significance. A p value of less than 0.05 was considered as significant. IHC staining and scoring for p53 protein on tissue microarray (TMA) was described in detail in (Tsao et al., 2007). Briefly, 4 μm sections from TMA were mounted onto slides. DO7 antibody for p53 (NovoCastra Laboratories) was diluted at 1:200 and applied to the sample, which was microwave-heated for antigen retrieval. The dilution was optimized a priori to ensure that there was no stain on normal tissue. Staining intensity was qualitatively scored from 0 (absent) to 3 (strong), and the percentage of tumor cells with nuclear staining was estimated. A sample with more than 15% cells with intensity scored 1 and above was defined as IHC positive.

Statistical Analysis

Unless otherwise specified, all p values were calculated using a two-tailed Student's t test in Graphpad Prism.

SUPPLEMENTAL INFORMATION

Supplemental Information includes Supplemental Experimental Procedures and seven figures and can be found with this article online at <http://dx.doi.org/10.1016/j.ccell.2015.09.009>.

AUTHOR CONTRIBUTIONS

Conceptualization, I.G.C. and M.B.Y.; methodology, I.G.C., S.M., C.J.B., E.R.C., and M.B.Y.; formal analysis, I.G.C., C.Q.Z. and M.B.Y.; investigation, I.G.C., K.A.M., S.M., C.Q.Z., E.R.C., and M.T.H.; resources, E.R.C., R.A.G., M.S.T., M.T.H., and M.B.Y.; data curation, I.G.C. and C.Q.Z.; writing- original draft, I.G.C. and M.B.Y.; writing- review and editing, K.A.M., S.M., C.Q.Z., M.S.T., M.T.H., and M.B.Y.; visualization, I.G.C. and C.Q.Z.; supervision, I.G.C., M.T.H., and M.B.Y.; project administration, I.G.C. and M.B.Y.; funding acquisition, I.G.C. and M.B.Y.

ACKNOWLEDGMENTS

We wish to thank Drs. Kirsty Sawicka, Pau Creixell, Scott Floyd, Michael Lee, Christian Ellson, and all members of the M.T.H. and M.B.Y. labs for helpful advice and discussions. We thank the Swanson Biotechnology Center, especially the applied therapeutics and whole animal imaging facility (Scott Malstrom and Milton Cornwall-Brady), flow cytometry facility, and the Barbara K. Ostrom Bioinformatics & Computing Facility (Charlie Whittaker) at the Koch Institute/MIT. This work was supported by the Austrian Science Fund (FWF) (J 2900-B21 to S.M.), the German Cancer Foundation (Mildred-Scheel Fellowship to C.J.B.), the Damon Runyon Cancer Research Foundation (DRG 2127-12 to K.A.M.), Canadian Cancer Society Research Institute (grant no. 020527 to M.S.T.), NIH grants (ES015339, GM60594, GM59281, CA112967), the Koch Institute and Center for Environmental Health Sciences Core Grants (P30-CA14051, ES-002109 to M.B.Y.), the Holloway Foundation (to M.B.Y.), and the Anna Fuller Fund (to I.G.C.). The authors wish to dedicate this paper to the memory of Officer Sean Collier for his caring service to the MIT.

Received: November 1, 2013

Revised: December 24, 2014

Accepted: September 18, 2015

Published: October 22, 2015

REFERENCES

- Abdelmohsen, K., Pullmann, R., Jr., Lal, A., Kim, H.H., Galban, S., Yang, X., Blethrow, J.D., Walker, M., Shubert, J., Gillespie, D.A., et al. (2007). Phosphorylation of HuR by Chk2 regulates SIRT1 expression. *Mol. Cell* 25, 543–557.
- Bartkova, J., Rezaei, N., Liontos, M., Karakaidos, P., Kletsas, D., Issaeva, N., Vassiliou, L.-V.F., Kolettas, E., Niforou, K., Zoumpourlis, V.C., et al. (2006). Oncogene-induced senescence is part of the tumorigenesis barrier imposed by DNA damage checkpoints. *Nature* 444, 633–637.
- Beli, P., Lukashchuk, N., Wagner, S.A., Weinert, B.T., Olsen, J.V., Baskcomb, L., Mann, M., Jackson, S.P., and Choudhary, C. (2012). Proteomic investigations reveal a role for RNA processing factor THRAP3 in the DNA damage response. *Mol. Cell* 46, 212–225.
- Buck, S.B., Bradford, J., Gee, K.R., Agnew, B.J., Clarke, S.T., and Salic, A. (2008). Detection of S-phase cell cycle progression using 5-ethynyl-2'-deoxyuridine incorporation with click chemistry, an alternative to using 5-bromo-2'-deoxyuridine antibodies. *Biotechniques* 44, 927–929.
- Cannell, I.G., Kong, Y.W., Johnston, S.J., Chen, M.L., Collins, H.M., Dobbyn, H.C., Elia, A., Kress, T.R., Dickens, M., Clemens, M.J., et al. (2010). p38 MAPK/MK2-mediated induction of miR-34c following DNA damage prevents Myc-dependent DNA replication. *Proc. Natl. Acad. Sci. USA* 107, 5375–5380.
- Cheek, C.F., Verma, C.S., Baselga, J., and Lane, D.P. (2011). Translating p53 into the clinic. *Nat. Rev. Clin. Oncol.* 8, 25–37.
- Ciccia, A., and Elledge, S.J. (2010). The DNA damage response: making it safe to play with knives. *Mol. Cell* 40, 179–204.
- Cuadrado, M., Gutierrez-Martinez, P., Swat, A., Nebreda, A.R., and Fernandez-Capetillo, O. (2009). p27Kip1 stabilization is essential for the maintenance of cell cycle arrest in response to DNA damage. *Cancer Res.* 69, 8726–8732.
- Darnell, R.B. (2010). HITS-CLIP: panoramic views of protein-RNA regulation in living cells. *Wiley Interdiscip. Rev. RNA* 7, 266–286.
- Doles, J., Oliver, T.G., Cameron, E.R., Hsu, G., Jacks, T., Walker, G.C., and Hemann, M.T. (2010). Suppression of Rev3, the catalytic subunit of Pol ζ , sensitizes drug-resistant lung tumors to chemotherapy. *Proc. Natl. Acad. Sci. USA* 107, 20786–20791.
- Frescas, D., and Pagano, M. (2008). Deregulated proteolysis by the F-box proteins SKP2 and β -TrCP: tipping the scales of cancer. *Nat. Rev. Cancer* 8, 438–449.
- Hafner, M., Landthaler, M., Burger, L., Khorshid, M., Hausser, J., Berninger, P., Rothballer, A., Ascano, M., Jr., Jungkamp, A.-C., Munschauer, M., et al. (2010). Transcriptome-wide identification of RNA-binding protein and microRNA target sites by PAR-CLIP. *Cell* 141, 129–141.

- Hsieh, F.F., Barnett, L.A., Green, W.F., Freedman, K., Matushansky, I., Skoultschi, A.I., and Kelley, L.L. (2000). Cell cycle exit during terminal erythroid differentiation is associated with accumulation of p27(Kip1) and inactivation of cdk2 kinase. *Blood* 96, 2746–2754.
- Jackson, S.P., and Bartek, J. (2009). The DNA-damage response in human biology and disease. *Nature* 461, 1071–1078.
- Jackson, E.L., Olive, K.P., Tuveson, D.A., Bronson, R., Crowley, D., Brown, M., and Jacks, T. (2005). The differential effects of mutant p53 alleles on advanced murine lung cancer. *Cancer Res.* 65, 10280–10288.
- Kedde, M., Strasser, M.J., Boldajipour, B., Oude Vrielink, J.A.F., Slanchev, K., le Sage, C., Nagel, R., Voorhoeve, P.M., van Duijse, J., Ørom, U.A., et al. (2007). RNA-binding protein Dnd1 inhibits microRNA access to target mRNA. *Cell* 131, 1273–1286.
- Kedde, M., van Kouwenhove, M., Zwart, W., Oude Vrielink, J.A.F., Elkon, R., and Agami, R. (2010). A Pumilio-induced RNA structure switch in p27-3' UTR controls miR-221 and miR-222 accessibility. *Nat. Cell Biol.* 12, 1014–1020.
- Keene, J.D., Komisarow, J.M., and Friedersdorf, M.B. (2006). RIP-Chip: the isolation and identification of mRNAs, microRNAs and protein components of ribonucleoprotein complexes from cell extracts. *Nat. Protoc.* 1, 302–307.
- Kelland, L. (2007). The resurgence of platinum-based cancer chemotherapy. *Nat. Rev. Cancer* 7, 573–584.
- Liontos, M., Velimezi, G., Pateras, I.S., Angelopoulou, R., Papavassiliou, A.G., Bartek, J., and Gorgoulis, V.G. (2010). The roles of p27(Kip1) and DNA damage signaling in the chemotherapy-induced delayed cell cycle checkpoint. *J. Cell. Mol. Med.* 14, 2264–2267.
- Matsuoka, S., Ballif, B.A., Smogorzewska, A., McDonald, E.R., 3rd, Hurov, K.E., Luo, J., Bakalarski, C.E., Zhao, Z., Solimini, N., Lerenthal, Y., et al. (2007). ATM and ATR substrate analysis reveals extensive protein networks responsive to DNA damage. *Science* 316, 1160–1166.
- Morandell, S., Reinhardt, H.C., Cannell, I.G., Kim, J.S., Ruf, D.M., Mitra, T., Couvillon, A.D., Jacks, T., and Yaffe, M.B. (2013). A reversible gene-targeting strategy identifies synthetic lethal interactions between MK2 and p53 in the DNA damage response in vivo. *Cell Rep.* 5, 868–877.
- Olive, K.P., Tuveson, D.A., Ruhe, Z.C., Yin, B., Willis, N.A., Bronson, R.T., Crowley, D., and Jacks, T. (2004). Mutant p53 gain of function in two mouse models of Li-Fraumeni syndrome. *Cell* 119, 847–860.
- Paulsen, R.D., Soni, D.V., Wollman, R., Hahn, A.T., Yee, M.-C., Guan, A., Hesley, J.A., Miller, S.C., Cromwell, E.F., Solow-Cordero, D.E., et al. (2009). A genome-wide siRNA screen reveals diverse cellular processes and pathways that mediate genome stability. *Mol. Cell* 35, 228–239.
- Polyak, K., Lee, M.H., Erdjument-Bromage, H., Koff, A., Roberts, J.M., Tempst, P., and Massagué, J. (1994). Cloning of p27Kip1, a cyclin-dependent kinase inhibitor and a potential mediator of extracellular antimitogenic signals. *Cell* 78, 59–66.
- Reinhardt, H.C., Aslanian, A.S., Lees, J.A., and Yaffe, M.B. (2007). p53-deficient cells rely on ATM- and ATR-mediated checkpoint signaling through the p38MAPK/MK2 pathway for survival after DNA damage. *Cancer Cell* 11, 175–189.
- Reinhardt, H.C., Hasskamp, P., Schmedding, I., Morandell, S., van Vugt, M.A.T.M., Wang, X., Linding, R., Ong, S.-E., Weaver, D., Carr, S.A., and Yaffe, M.B. (2010). DNA damage activates a spatially distinct late cytoplasmic cell-cycle checkpoint network controlled by MK2-mediated RNA stabilization. *Mol. Cell* 40, 34–49.
- Reinhardt, H.C., Cannell, I.G., Morandell, S., and Yaffe, M.B. (2011). Is post-transcriptional stabilization, splicing and translation of selective mRNAs a key to the DNA damage response? *Cell Cycle* 10, 23–27.
- Rousseau, S., Morrice, N., Peggie, M., Campbell, D.G., Gaestel, M., and Cohen, P. (2002). Inhibition of SAPK2a/p38 prevents hnRNP A0 phosphorylation by MAPKAP-K2 and its interaction with cytokine mRNAs. *EMBO J.* 21, 6505–6514.
- Shyu, A.B., and Wilkinson, M.F. (2000). The double lives of shuttling mRNA binding proteins. *Cell* 102, 135–138.
- Socinski, M.A. (2004). Cytotoxic chemotherapy in advanced non-small cell lung cancer: a review of standard treatment paradigms. *Clin. Cancer Res.* 10, 4210s–4214s.
- Sturn, A., Quackenbush, J., and Trajanoski, Z. (2002). Genesis: cluster analysis of microarray data. *Bioinformatics* 18, 207–208.
- Sweet-Cordero, A., Mukherjee, S., Subramanian, A., You, H., Roix, J.J., Ladd-Acosta, C., Mesirov, J., Golub, T.R., and Jacks, T. (2004). An oncogenic KRAS2 expression signature identified by cross-species gene-expression analysis. *Nat. Genet.*
- Toyoshima, H., and Hunter, T. (1994). p27, a novel inhibitor of G1 cyclin-Cdk protein kinase activity, is related to p21. *Cell* 78, 67–74.
- Tsao, M.S., Aviel-Ronen, S., Ding, K., Lau, D., Liu, N., Sakurada, A., Whitehead, M., Zhu, C.Q., Livingston, R., Johnson, D.H., et al. (2007). Prognostic and predictive importance of p53 and RAS for adjuvant chemotherapy in non small-cell lung cancer. *J. Clin. Oncol.* 25, 5240–5247.
- Wang, Y., Xiao, X., Zhang, J., Choudhury, R., Robertson, A., Li, K., Ma, M., Burge, C.B., and Wang, Z. (2013). A complex network of factors with overlapping affinities represses splicing through intronic elements. *Nat. Struct. Mol. Biol.* 20, 36–45.
- Winton, T., Livingston, R., Johnson, D., Rigas, J., Johnston, M., Butts, C., Cormier, Y., Goss, G., Incelet, R., Vallieres, E., et al.; National Cancer Institute of Canada Clinical Trials Group; National Cancer Institute of the United States Intergroup JBR.10 Trial Investigators (2005). Vinorelbine plus cisplatin vs. observation in resected non-small-cell lung cancer. *N. Engl. J. Med.* 352, 2589–2597.
- Yemelyanova, A., Vang, R., Kshirsagar, M., Lu, D., Marks, M.A., Shih, I.M., and Kurman, R.J. (2011). p53 IHC ovarian cancer. *Mod. Pathol.* 24, 1248–1253.
- Zhu, C.Q., Ding, K., Strumpf, D., Weir, B.A., Meyerson, M., Pennell, N., Thomas, R.K., Naoki, K., Ladd-Acosta, C., Liu, N., et al. (2010). Prognostic and predictive gene signature for adjuvant chemotherapy in resected non-small-cell lung cancer. *J. Clin. Oncol.* 28, 4417–4424.